

Received Date: 25-aug-2016

Revised Date: 30-sep-2016

Accepted Date: 03-oct-2016

Article Type: Full Paper

## On-Surface Metalation and 2D Self-Assembly of Pyrphyrin Molecules Into Metal-Coordinated Networks on Cu(111)

Jingyi Li,<sup>a</sup> Christian Wäckerlin,<sup>a,\*</sup> Stephan Schnidrig,<sup>b</sup> Evelyne Joliat,<sup>b</sup> Roger Alberto,<sup>b</sup> Karl-Heinz Ernst,<sup>a,b,\*</sup>

<sup>a</sup> Empa, Swiss Federal Laboratories for Materials Science and Technology,  
Überlandstrasse 129, 8600 Dübendorf, Switzerland, e-mail christian.waeckerlin@empa.ch, karl-heinz.ernst@empa.ch

<sup>b</sup> Institut für Chemie, Universität Zürich, CH-8057 Zürich, Switzerland

The metalation of the tetradentate molecule pyrphyrin by copper substrate atoms on a Cu(111) surface is studied. Pyrphyrin, in contrast to porphyrin, consists of four fused pyridine groups instead of pyrrol groups. Using thermal desorption spectroscopy (TDS) and N 1s X-ray photoelectron spectroscopy (XPS), we show that metalation of the monolayer of pyrphyrin with Cu adatoms from the Cu(111) surface occurs at 377 K. The formation of an extended two-dimensional (2D) network is observed with scanning tunneling microscopy (STM). A honeycomb-like lattice of metalated pyrphyrin molecules is formed by intermolecular connection *via* the two cyano groups at the periphery of pyrphyrin as well as Cu adatoms. Dehydrogenation at the periphery of the molecule is observed during annealing at 520 K. The surface adsorbed metal-pyrphyrin has the potential to serve as a molecular catalyst.

**Keywords:** 2D metal coordination • scanning tunneling microscopy • pyrphyrin • surface self-assembly

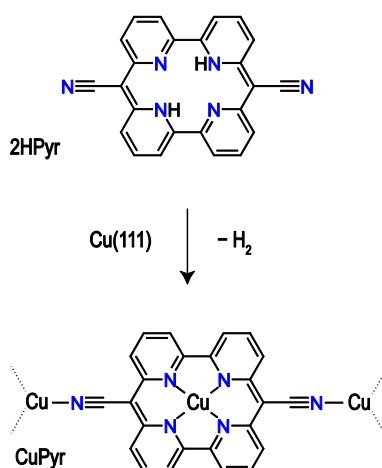
### Introduction

Surface functionalization with macrocycles, such as porphyrin or phthalocyanine, presents a fascinating platform for studying physical and chemical phenomena at interfaces and provides the basis for many applications. These predominantly planar macrocycles can coordinate a metal ion, rendering them interesting model systems to study coordination chemistry at surfaces.<sup>[1–5]</sup> In addition, the central metal ions can coordinate an axial ligand at the site opposite to the surface.<sup>[6,7]</sup> For example, this has led to the demonstration of special catalytic properties for water oxidation on porphyrin derived 2D layers containing different transition metals.<sup>[8]</sup> An attractive alternative to the deposition of metal containing macrocycles is to perform the coordination of a metal atom (*i.e.* metalation) *in-situ* directly at the

This document is the accepted manuscript version of the following article: Li, J., Wäckerlin, C., Schnidrig, S., Joliat, E., Alberto, R., & Ernst, K.-H. (2017). On-surface metalation and 2D self-assembly of pyrphyrin molecules into metal-coordinated networks on Cu(111). *Helvetica Chimica Acta*, 100(1), e1600278 (8 pp.). <http://doi.org/10.1002/hlca.201600278>

surface under ultrahigh vacuum (UHV) conditions. The metal atoms can be provided either by the surface (sometimes termed as 'self-metalation') or supplied by co-deposition through evaporation.<sup>[9,20,2-5]</sup>

In this work, we report the on-surface chemistry of the macrocycle pyrphyrin (2HPyr, Scheme 1) on the copper(111) surface. In contrast to molecules from the tetrapyrrole family, such as porphyrin or phthalocyanine, the pyrphyrin macrocycle consists of four fused pyridines instead of pyrroles.<sup>[11,12]</sup> Specifically, two 2,2'-bipyridine subunits are bridged by cyano-methylene units to form a plane consisting of two iminic (=N-) and two pyridinic (-NH-) nitrogens. Compared to porphyrin with 16 atoms in the inner macrocycle (12C + 4N), 2HPyr has there only 14 atoms (10C + 4N). After dehydrogenation of free base 2HPyr, the planar tetradentate pyrphyrin ligand can coordinate ions such as Zn(II),<sup>[13,14]</sup> Mn(III)Cl<sup>[15]</sup> and Co(II)<sup>[12]</sup>. The on-surface formation of CoPyr has been achieved previously on the Au(111) surface in presence of Co adatoms.<sup>[16]</sup> In solution, CoPyr derived complexes have been shown to catalyze the reduction of water under illumination with light.<sup>[12]</sup> Cyano-functionalized molecules in general may also act as ligands for surface adatoms.<sup>[17-21]</sup> Such coordination at radial or terminal functional groups leads often to the formation of highly ordered 2D metal-organic coordination networks.<sup>[22-24]</sup>



Scheme 1. Metalation of 2HPyr to CuPyr. The cyano groups can also coordinate transition metal atoms, thereby bridging several molecules into a 2D metal-organic layer.

## Results and Discussion

Submonolayer coverages of 2HPyr were obtained by sublimation in UHV on clean Cu(111) single crystal substrates (*cf.* Experimental section). Here, one monolayer (ML) is defined as the most densely packed layer achieved by Pyr molecules on the Cu(111) surface without any molecules in a second layer. The molecular coverage was tuned by the evaporation time and monitored with X-ray photoelectron spectroscopy (XPS) by comparing the intensity ratio of Cu 2p<sub>3/2</sub> and C 1s peaks and calibration of the absolute coverage using scanning tunneling microscopy (STM).

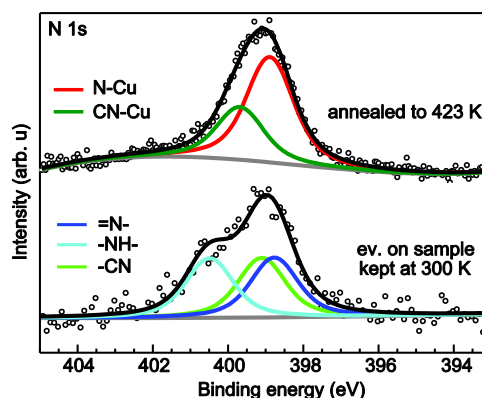


Figure 1. XP spectra in the N 1s peak region revealing the metalation reaction of 2HPyr to CuPyr (1.0 ML). After deposition, the N1s signal can be deconvoluted into 3 components, *i.e.* iminic ( $-\text{NH}-$ , 400.5 eV), pyridinic ( $=\text{N}-$ , 398.8 eV) and cyano ( $\text{C}\equiv\text{N}$ , 399.1 eV) nitrogen. The narrower N 1s peak observed after annealing can be deconvoluted into N-Cu (398.9 eV) and  $\text{C}\equiv\text{N}-\text{Cu}$  (399.8 eV) species at 4:2 peak area ratio, respectively. The background of the clean sample was subtracted.

For 1.0 ML of 2HPyr deposited on Cu(111) kept at room temperature (RT, 295 K), XP spectra (Figure 1) reveal an N 1s signal with two distinctive peaks. This is consistent with the 3 nitrogen species present in 2HPyr, *i.e.* for pyridinic nitrogen ( $-\bar{\text{N}}\text{H}-$ ) at 400.5 eV, iminic nitrogen ( $=\bar{\text{N}}-$ ) at 398.8 eV, and the cyano nitrogen ( $-\text{C}\equiv\text{N}|$ ) at 399.1 eV binding energy, with a peak area ratio of 2:2:2. The assigned binding energies are consistent with the literature for 2HPyr<sup>[16]</sup>, free base tetraphenylporphyrin (2HTPP) and cyano-functionalized molecules at monolayer coverage on various metal surfaces.<sup>[2,4,28]</sup> After annealing to 473 K for 10 min, a narrower N 1s peak is observed which can be deconvoluted into N-Cu (398.9 eV) and a  $\text{C}\equiv\text{N}-\text{Cu}$  (399.8 eV) signals at 4:2 peak area ratio, respectively.<sup>[9,18,25,26]</sup> This feature is characteristic for the dehydrogenation of two imino groups in the molecular core due to the incorporation of a Cu atom in the macrocycle, leading to four equivalent nitrogen atoms. The binding energies agree with previous results on porphyrin metalation on copper surfaces<sup>[25]</sup> and with CoPyr on Au(111).<sup>[16]</sup> Remarkably, the  $\text{C}\equiv\text{N}$  component shifts towards a higher binding energy by 0.7 eV indicating a significant modification of the cyano groups' chemical environment, namely, a more positively charged N-atom due to the additional bond to a Cu atom. A similar N 1s peak shift has been observed after coordination of Cu adatoms to cyanohelicene derivatives.<sup>[18]</sup> Hence, the shift of the cyano-N indicates that Cu coordination at the cyano groups also occurs for porphyrin on Cu(111) upon annealing.

By measuring the evolution of molecular hydrogen using thermal desorption spectroscopy (TDS) further insight into the process of metalation is gained. Ramping the temperature at a rate of  $3\text{ K s}^{-1}$ , two distinct  $\text{H}_2$  desorption maxima  $\alpha$  and  $\beta$  are observed in the mass spectrometer at 377 K and 696 K, respectively (Figure 2). The spectrum obtained on clean Cu(111) under identical conditions does not exhibit these features, because hydrogen from the residual gas does not adsorb on copper at RT. Based on the observation of complete metalation with XPS after annealing to 423 K, we assign the  $\alpha$  peak to the dehydrogenation reaction of the pyridinic nitrogen atoms during metalation, which is consistent with observations of porphyrin metalation on Cu(111) reported in the literature.<sup>[4,27,28]</sup> Considering the heating rate of the TDS experiment, this means that the metalation of 2HPyr on Cu(111) occurs at 377 K within seconds.

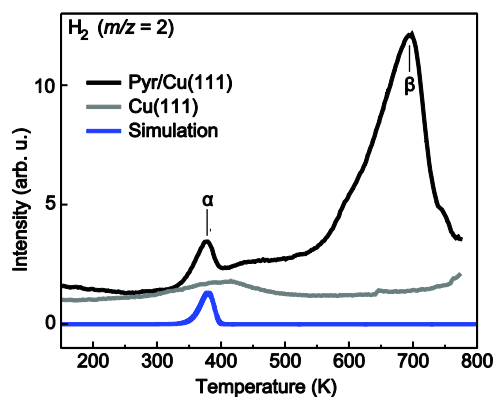


Figure 2. Thermal desorption spectra for molecular hydrogen ( $m/z = 2$ ) obtained for 1.2 ML of 2HPyr deposited on Cu(111) kept at 110 K. The temperature ramp rate is  $3\text{ K s}^{-1}$ . Two distinct maxima  $\alpha$  and  $\beta$  are observed at 377 K and 696 K, which are assigned to  $\text{H}_2$  desorbing during metalation and dehydrogenation of the carbon backbone, respectively.

The intense and broad TDS  $\beta$  peak is assigned to dehydrogenation at the periphery of the molecule, *i.e.* C-H bond breaking. Its broad shape means that this reaction occurs over a wide temperature range, which is explained by the non-equivalence of the peripheral hydrogens. Such pyrolysis is a common feature for adsorbed hydrocarbons that are too tightly bound to the surface to become desorbed intact. This process has also been observed for monolayers of tetrapyrroles adsorbed on metal surfaces.<sup>[25,27,29-31]</sup>

The energy barrier for the dehydrogenation of the porphyrin core and therefore for metalation can be obtained by numerically propagating the Polanyi-Wigner equation for increasing temperatures (see Experimental section). For simplicity we keep the attempt frequency  $\nu_0$  fixed to  $10^{15} \text{ s}^{-1}$ , which has been obtained by *Ditze et al.* for metalation of 2HTPP on Cu(111).<sup>[28]</sup> Assuming first-order kinetics, the simulation of peak  $\alpha$  (Figure 2) delivers best results (peak maximum temperature and peak shape) for an activation energy of 113 kJ/mol. This is substantially lower than observed for monolayers of 2HTPP on Cu(111), where the activation energy for the rate limiting step, *i.e.* incorporation of the Cu adatom into the macrocycle,<sup>[4]</sup> has been reported as high as 143 kJ/mol<sup>[28]</sup> and 134 kJ/mol,<sup>[27]</sup> using the same attempt frequency of  $\nu_0 = 10^{15} \text{ s}^{-1}$ . The smaller cavity of porphyrin may lead to a higher metal-ligand binding energy, but our method determines only the activation energy of the process, which includes also hydrogen release, recombination and desorption. Because recombinant hydrogen desorption occurs at much lower temperatures on Cu(111), the latter two steps must proceed very fast and the rate-limiting step must be assigned to the hydrogen release and Cu atom incorporation. Consequently, the lower activation energy must be attributed to a stronger surface interaction of 2HPyr, favoring the dissociation of the two H atoms from the molecule. Considering the lack of sterically demanding groups, which would keep a larger distance of the macrocycle from the surface (as in 2HTPP for example), this lower activation barrier for metalation of 2HPyr seems consistent with the assumed small distance to the surface. However, the slightly smaller cavity of 2HPyr compared to porphyrins does not appear to strongly affect the metalation temperature. Also note that the temperature for metalation has been shown to depend on the coverage, as this can modulate the distance of the molecule with respect to the surface, as reported for 2HTPP on Cu(111).<sup>[26]</sup> For the monolayer of the plain porphyrin-core species 2H-porphine and a submonolayer sample of 2H-phthalocyanine on Cu(111), the onset for metalation was reported at 373 K<sup>[32]</sup> and 240 K, respectively.<sup>[33]</sup> There, the low temperature for porphine metalation has also been attributed to an increased interaction with the surface due to a lower height above the surface.<sup>[4]</sup>

In order to investigate the structural changes of the molecules in the monolayer we performed STM investigations below metalation temperature and after annealing the adsorbate system above metalation temperature and above the temperature of periphery-dehydrogenation. Figure 3 displays STM images obtained for a 1.05 ML of 2HPyr deposited at RT surface temperature. Under these conditions, the molecules are not metalated. Using STM, we observe self-assembled domains as well as disordered areas. The streaks along the fast STM (horizontal) scan direction in the disordered areas are an indication for high partial mobility of molecules. Indeed, in subsequently recorded images we observe the attachment and detachment of molecules to and from the self-assembled arrays (see Figure S1 in Supporting Information). The hexagonal symmetry of self-assembled domains reflects the symmetry of the Cu(111) top surface layer. The molecules appear approximately square shaped with a depression in the center. Note that in STM, when operated in constant current mode, parts of a molecule farther away from the surface are coded with such relative higher brightness. As the cyano groups are not resolved, the exact orientation of each molecule cannot be determined. Some molecules appear fuzzy and roundish, presumably due to thermally induced rotation. The STM appearance of the molecules and the mode of self-assembly is quite similar to 2HPyr on Au(111).<sup>[16]</sup>

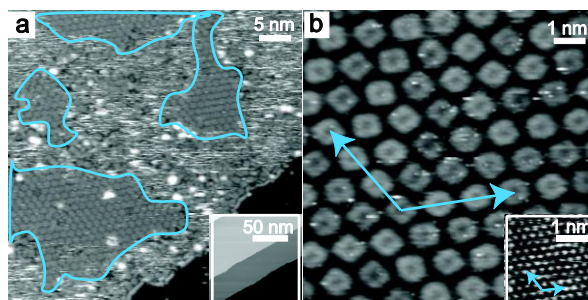


Figure 3. STM images of 1.05 ML of 2HPyr deposited on Cu(111) at 295 K and of the clean surface (insets). (a) Self-assembled domains (framed with blue lines) of molecules coexist with disordered areas ( $U = 1.28 \text{ V}$ ,  $I = 20 \text{ pA}$ ,  $T = 295 \text{ K}$ ). Streaks appear along the fast scan direction (horizontal) in the disordered areas, indicating that some molecules are mobile. (b) Small scale image ( $U = 0.94 \text{ V}$ ,  $I = 20 \text{ pA}$ ,  $T = 295 \text{ K}$ ) showing the molecules in a self-assembled domain. The insets display an overview image (inset in a,  $U = 1.25 \text{ V}$ ,  $I = 60 \text{ pA}$ ,  $T = 295 \text{ K}$ ) and atomic resolution (inset in b,  $U = -4.6 \text{ mV}$ ,  $I = -2.9 \text{ nA}$ ,  $T = 295 \text{ K}$ ), respectively. Blue arrows indicate unit-cell vectors ( $\times 3$  for better visibility) of the clean surface and the molecular layer, respectively.

Figure 4 shows STM images of metalated Pyr on Cu(111). The sample has been obtained after deposition of 0.7 ML 2HPyr at 295 K, annealed to 423 K for 10 min and recorded at 130 K due to too high surface mobility at room temperature. The overview (Figure 4a) reveals that metalated molecules assemble predominantly into a honeycomb lattice. The chain and honeycomb motives consist of two or three cyano groups coordinating a Cu adatom. About 10% of the surface is covered by molecular chains (framed in blue). Such chain morphology has been also observed for molecules with two cyano groups attached at opposite sides of the same molecule.<sup>[17–21]</sup> At a higher coverage, the chain motif has been replaced by the denser honeycomb motif.<sup>[19]</sup> Therefore, we conclude that the coexistence of chain and honeycomb motifs is due to the coverage being slightly too low for the pure honeycomb phase.<sup>[19]</sup> We did not observe a four-fold (or higher) coordination motif,<sup>[23]</sup> which seems sterically impossible in a purely 2D motif.

Interestingly, both the formation of an adatom stabilized honeycomb network and the shift to higher binding energy of the cyano N1s XP signal has not been observed for 2HPyr/Au(111) after metalation with Co atoms.<sup>[16]</sup> This may be due to the presence of too small amounts of Co for both metalation and cyano-coordination or it may reflect a more profound difference between the two-molecule/adatom/substrate systems.

Some pores of the honeycomb lattice, as marked by blue arrows in Figure 4b and 4c, are filled with an additional molecule. For these molecules, the rectangular shape of pyrphyrin is not resolved, but still they appear with the same contrast, including the depression in the center. This difference in appearance is explained by continuous hopping of the rectangular molecule between identical orientations in the hexagonal pore.<sup>[34]</sup> The reason for this 'rotation' is explained by the lack of coordination of the additional molecules in the pores. While the molecules of the honeycomb network are coordinated via the three fold Cu-nodes, an additional molecule in the pore does not have such possibility of intermolecular binding. Few pores of the honeycomb lattice appear differently, that is, they show bright three-lobe protrusions (Figure 4b, red arrow). However, the nature of this appearance remains unclear.

In the constant current STM mode used in this work, the height of the tip above the sample is continuously controlled to keep the tunneling current at the set point value. Therefore the dark appearance in the center of the molecules is due to a reduced overlap of orbitals at the tip and the surface, resulting in a lower tunneling probability and therefore a smaller tip sample distance which is coded dark in the images. The dark appearance of the center of the molecules therefore implies the absence of 3d states with predominantly out-of-plane character close to the Fermi level,<sup>[35,36]</sup> consistent with the presence of a Cu in the center of the molecule. In contrast, Co in CoPyr/Au(111) were imaged as high (coded bright) protrusions, consistent with the presumed presence of out-of-plane 3d states in 3d<sup>7</sup> low-spin Co.<sup>[16]</sup>

Due to the robust nature of the honeycomb lattice, we were able to obtain images with very small bias voltages and high tunneling currents. Under these conditions, the STM tip approaches close to the molecule, thereby increasing the intramolecular resolution and permitting tunneling into in-plane orbitals.<sup>[37]</sup> Figure 5 exhibits a series of STM images obtained at a bias voltage of 57 mV and tunneling currents increasing from 40 pA to ~2 nA. At a larger tip sample distance (*i.e.* low tunneling currents) the image resolution is lower. This is also reflected in the larger appearance of the molecules at low tunnel currents. At tunneling currents above 500 pA, a small protrusion inside of a depression becomes visible (Figure 5d-f). Such a small protrusion inside of a depression was also observed in STM experiments on Cu-porphine at low bias voltage and high tunneling current.<sup>[38]</sup> We tentatively identify this contrast to tunneling into in-plane orbitals of Cu enabled by the smaller tip-sample distance.

The third regime identified by XPS and TDS corresponds to molecules that are partially dehydrogenated at the periphery. The onset of this pyrolysis, as observed with TDS at seconds-time scale, is at ~550 K. Hence, we deposited molecules onto the sample kept at 520 K, accounting for the substantially longer deposition times (20 min/ML). Under these conditions a significantly different morphology of the dehydrogenated CuPyr molecules is observed (Figure 6). The molecules appear then with slightly irregular shapes and regular self-assembly is absent. A similar appearance was also observed for tetrapyrrole monolayers on Cu and Ag substrates which also dehydrogenated at the periphery by annealing to 500 – 640 K.<sup>[25,27,29–31]</sup>

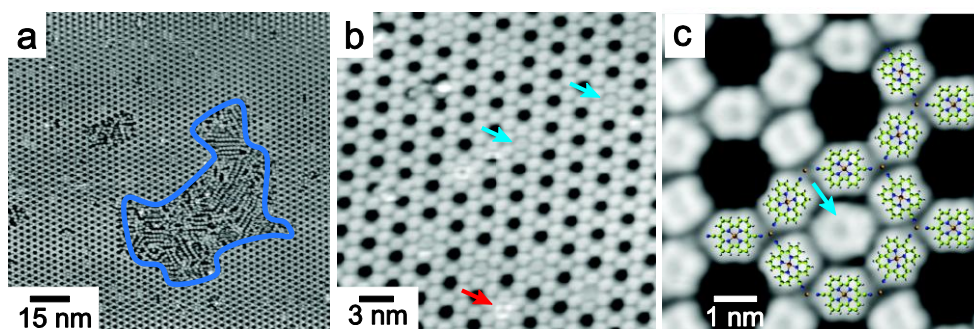


Figure 4. STM images of 0.7 ML 2HPyr after annealing to 423 K. The large scale image (a,  $U = 58$  mV,  $I = 17$  pA,  $T = 130$  K) exhibits an extended honeycomb porous network. Small domains with linearly coordinated molecules, appearing as chains, are also present (framed by a blue line). An image at larger magnification (b,  $U = 363$  mV,  $I = 20$  pA,  $T = 130$  K) shows that some pores of the honeycomb lattice are filled with molecules (indicated by blue arrows). These molecules do not have the distinct square shape, but seem to rotate even at 130 K. Some pores show bright three-lobe features (red arrow), whose identity is unclear. A superposition of the molecular structure and Cu adatoms involved with an STM image (c,  $U = 57$  mV,  $I = 230$  pA,  $T = 130$  K) illustrates the structure of the metal-organic honeycomb lattice.

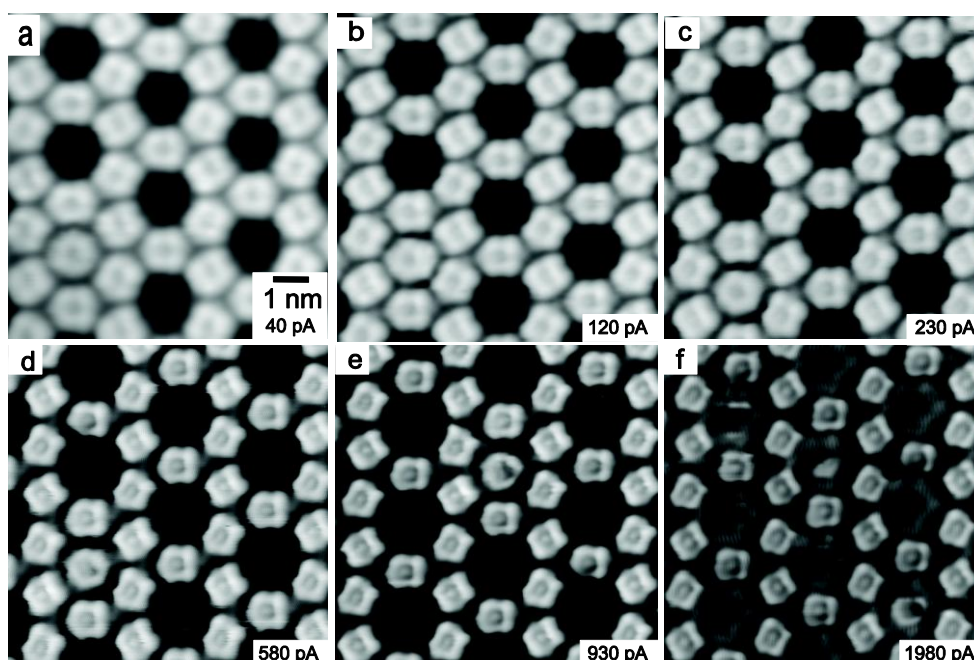


Figure 5. STM images for a 0.7 ML 2HPyr layer after annealing to 423 K at different tunneling currents ( $U = 57$  mV,  $T = 130$  K). With increasing tunneling current the STM operates with the tip closer to the surface, resulting in a more localized tunneling process. This allows that more intramolecular details are resolved and the molecules appear smaller. At high current set points (>500 pA) a small protrusion becomes visible in the depression in the center of the molecule. The images do not necessarily display the same spot on the surface. Each image shows one honeycomb pore which is filled by an additional molecule. The scale bar in (a) applies to all images.

Finally, we present direct evidence that the metalation of 2HPyr on Cu(111) proceeds also into the multilayer (Figure 7). TD spectra obtained at  $m/z$  ratios 386 (2HPyr) and 447 (CuPyr) for  $\sim 3\text{--}5$  ML of 2HPyr deposited on Cu(111) clearly show that in part the free base, but also metalated CuPyr, desorb from the surface. We recall that CuPyr directly located on the metal surface is too strongly bound and undergoes dehydrogenation and decomposition. However, the TD spectra resolve both 2HPyr and CuPyr desorbing at around 550 K from the multilayer as intact molecules. Our results are consistent with the literature, where metalation in the multilayer has also been observed for tetrapyrroles.<sup>[33,38,39]</sup>

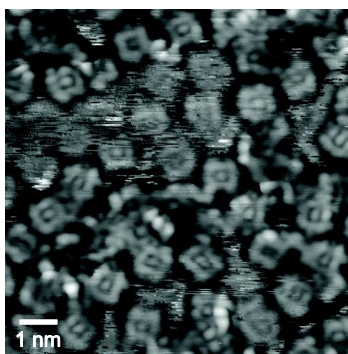


Figure 6. STM image ( $U = -1.0$  V,  $I = -2.8$  nA,  $T = 295$  K) acquired after deposition of the molecules (0.9 ML) onto a sample kept at 520 K, *i.e.* at temperatures where dehydrogenation occurs. The molecules appear in part as irregular shapes. No ordered self-assembly is observed.

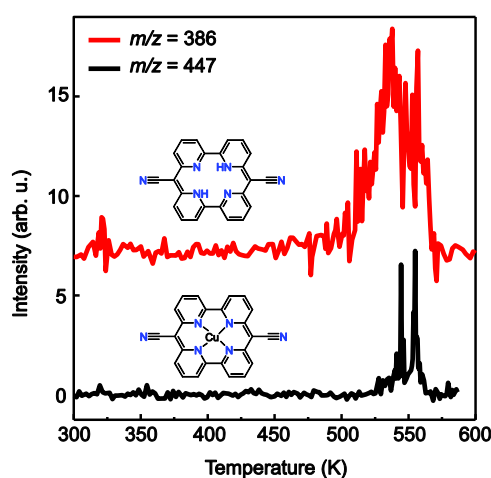


Figure 7. TD spectra for 2HPyr ( $m/z = 386$ ) and CuPyr ( $m/z = 447$ ) obtained on multilayers ( $\sim 3$ – $5$  ML) of 2HPyr on Cu(111). The heating rate is  $2$  K  $s^{-1}$ . Both 2HPyr and CuPyr are detected, demonstrating that the metalation does occur in part in the multilayer. The 2HPyr spectrum is offset along the intensity axis for clarity.

## Conclusions

The porphyrin-Cu(111) surface system shows a wealth of metal-organic chemistry, including on-surface metalation and formation of highly ordered metal-organic 2D layers with the molecules bridged by coordinated Cu adatoms. The metalation proceeds in part also into the multilayers. Our results show that concepts of surface functionalization and chemistry, like the on-surface metalation of macrocycles, that have been previously developed for porphyrines and phthalocyanines can be extended to systems with probably different functionality and specific catalytic activity.

## Experimental Part

### Sample preparation and analysis

The experiments were performed in ultrahigh vacuum (base pressure below  $3 \times 10^{-10}$  mbar). The Cu(111) surface was prepared by repeated cycles of Ar<sup>+</sup> sputtering and annealing to 723 K and cleanliness was checked by XPS and STM. 2HPyr was purified by re-sublimation in high vacuum ( $\sim 10^{-5}$  mbar), thoroughly degassed and sublimated from a Knudsen cell (583 K, rate:  $\sim 0.05$  ML  $min^{-1}$ ). For XPS

(Specs PHOIBOS 100), photoelectrons were excited using non-monochromatic Al K $\alpha$  X-rays and collected along the direction normal to the crystal surface. The spectra were calibrated using the Cu 2p $_{3/2}$  signal (932.7 eV) and the Fermi level (0.0 eV) of the crystal. STM images were recorded with the Specs Aarhus 150 instrument, in constant current mode with a PtIr (90% Pt) tip. The images were processed using the WSxM software<sup>[40]</sup> and calibrated using the atomic resolution of Cu(111). TDS was recorded with a differentially pumped quadrupole mass spectrometer (Balzers QME 200) and a thermocouple inserted into a hole in the side of the single crystal. The mass spectrometer was mounted in a housing equipped with a small pinhole in order to collect exclusively material desorbing from the surface.

### TDS Simulations

The simulations were performed by numerically propagating the Polanyi-Wigner equation (1)<sup>[41,42]</sup> on a linear temperature  $T$  ramp.

$$r = -\frac{d\theta}{dt} = \nu \theta^n \exp\left(-\frac{E}{RT}\right) \quad (1)$$

Here,  $E$  is the barrier height,  $\nu$ , the attempt frequency,  $n$  is the order of reaction and  $R$  is the gas constant. Using an initial coverage  $\theta$ , which is arbitrary for the first order kinetics used here, the reaction rate  $r(t)$  and the coverage  $\theta(t)$  are evaluated step-wise while increasing the temperature  $T$  with every step.  $10^4$  time steps were sufficient, *i.e.* more time steps did not affect the rate. For the case of desorption,  $r(t)$  corresponds to the TDS signal intensity.

### Acknowledgements

Financial support by the University Zürich research priority program LightChEC, the Schweizerischer Nationalfonds (R'Equip) and CCMX is gratefully acknowledged.

### Supporting Information

Supporting information for this article is available on the WWW under [http://dx.doi.org/\[DOI\]](http://dx.doi.org/[DOI]).

### Author Contribution Statement

J.L. and C.W. performed the experiments and analyzed the data. S.S., E.J. synthesized the molecules under supervision of R.A.. K-H.E. and R.A. perceived the experiments. J.L., C.W., and K.-H.E. wrote the paper with input from all authors.

### References

- [1] W. Auwärter, D. Écija, F. Klappenberger, J. V. Barth, 'Porphyrins at interfaces', *Nat. Chem.* **7** **2015**, 105–120.
- [2] J. M. Gottfried, 'Surface chemistry of porphyrins and phthalocyanines', *Surf. Sci. Rep.* **70** **2015**, 259–379.
- [3] H. Marbach, 'Surface-Mediated *in Situ* Metalation of Porphyrins at the Solid–Vacuum Interface', *Acc. Chem. Res.* **48** **2015**, 2649–2658.
- [4] K. Diller, A. C. Papageorgiou, F. Klappenberger, F. Allegretti, J. V. Barth, W. Auwärter, 'In vacuo interfacial tetrapyrrole metallation', *Chem. Soc. Rev.* **45** **2016**, 1629–1656.
- [5] M. Gottfried, H. Marbach, 'Surface-Confined Coordination Chemistry with Porphyrins and Phthalocyanines: Aspects of Formation, Electronic Structure, and Reactivity', *Z. Phys. Chem.* **223** **2009**, 53–74.
- [6] K. Flechtner, A. Kretschmann, H.-P. Steinrück, J. M. Gottfried, 'NO-Induced Reversible Switching of the Electronic Interaction between a Porphyrin-Coordinated Cobalt Ion and a Silver Surface', *J. Am. Chem. Soc.* **129** **2007**, 12110–12111.
- [7] N. Ballav, C. Wäckerlin, D. Siewert, P. M. Oppeneer, T. A. Jung, 'Emergence of On-Surface Magnetochemistry', *J. Phys. Chem. Lett.* **4** **2013**, 2303–2311.
- [8] B. Wurster, D. Grumelli, D. Hötger, R. Gutzler, K. Kern, 'Driving the Oxygen Evolution Reaction by Nonlinear Cooperativity in Bimetallic Coordination Catalysts', *J. Am. Chem. Soc.* **138** **2016**, 3623–3626.
- [9] J. M. Gottfried, K. Flechtner, A. Kretschmann, T. Lukaszcyk, H.-P. Steinrück, 'Direct Synthesis of a Metalloporphyrin Complex on a Surface', *J. Am. Chem. Soc.* **128** **2006**, 5644–5645.
- [10] W. Auwärter, A. Weber-Bargioni, S. Brink, A. Riemann, A. Schiffrin, M. Ruben, J. V. Barth, 'Controlled Metalation of Self-Assembled Porphyrin Nanoarrays in Two Dimensions', *ChemPhysChem* **8** **2007**, 250–254.
- [11] S. Ogawa, R. Narushima, Y. Arai, 'Aza Macrocycle that selectively binds lithium ion with color change', *J. Am. Chem. Soc.* **106** **1984**, 5760–5762.

- [12] E. Joliat, S. Schnidrig, B. Probst, C. Bachmann, B. Spingler, K. K. Baldridge, F. von Rohr, A. Schilling, R. Alberto, 'Cobalt complexes of tetradentate, bipyridine-based macrocycles: their structures, properties and photocatalytic proton reduction', *Dalton Trans.* 45 **2016**, 1737–1745.
- [13] R. Ibrahim, S. Tsuchiya, S. Ogawa, 'A Color-Switching Molecule: Specific Properties of New Tetraaza Macrocycle Zinc Complex with a Facile Hydrogen Atom', *J. Am. Chem. Soc.* 122 **2000**, 12174–12185.
- [14] Z. Zhu, K. Takano, A. Furuhashi, S. Ogawa, S. Tsuchiya, 'Theoretical Study of Geometries and Electronic Transition of Color-Switching Molecules: Tetra-Aza Macrocycle and Its Zinc Complexes', *Bull. Chem. Soc. Jpn.* 80 **2007**, 686–693.
- [15] C. Pierre, J.-M. Vincent, J.-B. Verlhac, C. Courseille, A. Dautant, C. Mathoniere, 'First synthesis and crystal structure of a Mn<sup>3+</sup> complex derived from the Ogawa porphyrin-like ligand', *New J. Chem.* 25 **2001**, 522–524.
- [16] G. Mette, D. Sutter, Y. Gurdal, S. Schnidrig, B. Probst, M. Iannuzzi, J. Hutter, R. Alberto, J. Osterwalder, 'From porphyrins to pyrphyrins: adsorption study and metalation of a molecular catalyst on Au(111)', *Nanoscale* 8 **2016**, 7958–7968.
- [17] G. Pawin, K. L. Wong, D. Kim, D. Sun, L. Bartels, S. Hong, T. S. Rahman, R. Carp, M. Marsella, 'A Surface Coordination Network Based on Substrate-Derived Metal Adatoms with Local Charge Excess', *Angew. Chem. Int. Ed.* 47 **2008**, 8442–8445.
- [18] A. Shchyrba, M.-T. Nguyen, C. Wäckerlin, S. Martens, S. Nowakowska, T. Ivas, J. Roose, T. Nijs, S. Boz, M. Schär, M. Stöhr, C. A. Pignedoli, C. Thilgen, F. Diederich, D. Passerone, T. A. Jung, 'Chirality Transfer in 1D Self-Assemblies: Influence of H-Bonding vs Metal Coordination between Dicyano[7]helicene Enantiomers', *J. Am. Chem. Soc.* 135 **2013**, 15270–15273.
- [19] G. E. Pacchioni, M. Pivetta, H. Brune, 'Competing Interactions in the Self-Assembly of NC–Ph<sub>3</sub>–CN Molecules on Cu(111)', *J. Phys. Chem. C* 119 **2015**, 25442–25448.
- [20] M. Pivetta, G. E. Pacchioni, E. Fernandes, H. Brune, 'Temperature-dependent self-assembly of NC–Ph<sub>3</sub>–CN molecules on Cu(111)', *J. Chem. Phys.* 142 **2015**, 101928.
- [21] F. Bischoff, Y. He, K. Seufert, D. Stassen, D. Bonifazi, J. V. Barth, W. Auwärter, 'Tailoring Large Pores of Porphyrin Networks on Ag(111) by Metal–Organic Coordination', *Chem. - Eur. J.* **2016**, DOI 10.1002/chem.201602154.
- [22] A. Dmitriev, H. Spillmann, N. Lin, J. V. Barth, K. Kern, 'Modular Assembly of Two-Dimensional Metal–Organic Coordination Networks at a Metal Surface', *Angew. Chem. Int. Ed.* 42 **2003**, 2670–2673.
- [23] J. V. Barth, G. Costantini, K. Kern, 'Engineering atomic and molecular nanostructures at surfaces', *Nature* 437 **2005**, 671–679.
- [24] J. V. Barth, 'Fresh perspectives for surface coordination chemistry', *Surf. Sci.* 603 **2009**, 1533–1541.
- [25] J. Xiao, S. Ditze, M. Chen, F. Buchner, M. Stark, M. Drost, H.-P. Steinrück, J. M. Gottfried, H. Marbach, 'Temperature-Dependent Chemical and Structural Transformations from 2H-tetraphenylporphyrin to Copper(II)-Tetraphenylporphyrin on Cu(111)', *J. Phys. Chem. C* 116 **2012**, 12275–12282.
- [26] M. Röckert, S. Ditze, M. Stark, J. Xiao, H.-P. Steinrück, H. Marbach, O. Lytken, 'Abrupt Coverage-Induced Enhancement of the Self-Metalation of Tetraphenylporphyrin with Cu(111)', *J. Phys. Chem. C* 118 **2014**, 1661–1667.
- [27] M. Röckert, M. Franke, Q. Tariq, D. Lungerich, N. Jux, M. Stark, A. Kaftan, S. Ditze, H. Marbach, M. Laurin, J. Libuda, H.-P. Steinrück, O. Lytken, 'Insights in Reaction Mechanistic: Isotopic Exchange during the Metalation of Deuterated Tetraphenyl-21,23 D-porphyrin on Cu(111)', *J. Phys. Chem. C* 118 **2014**, 26729–26736.
- [28] S. Ditze, M. Stark, M. Drost, F. Buchner, H.-P. Steinrück, H. Marbach, 'Activation Energy for the Self-Metalation Reaction of 2H-Tetraphenylporphyrin on Cu(111)', *Angew. Chem. Int. Ed.* 51 **2012**, 10898–10901.
- [29] C. Ruggieri, S. Rangan, R. A. Bartynski, E. Galoppini, 'Zinc(II) Tetraphenylporphyrin on Ag(100) and Ag(111): Multilayer Desorption and Dehydrogenation', *J. Phys. Chem. C* 120 **2016**, 7575–7585.
- [30] A. Wiengarten, J. A. Lloyd, K. Seufert, J. Reichert, W. Auwärter, R. Han, D. A. Duncan, F. Allegretti, S. Fischer, S. C. Oh, Ö. Sağlam, L. Jiang, S. Vijayaraghavan, D. Ćija, A. C. Papageorgiou, J. V. Barth, 'Surface-Assisted Cyclodehydrogenation; Break the Symmetry, Enhance the Selectivity', *Chem. - Eur. J.* 21 **2015**, 12285–12290.
- [31] O. Snezhkova, F. Bischoff, Y. He, A. Wiengarten, S. Chaudhary, N. Johansson, K. Schulte, J. Knudsen, J. V. Barth, K. Seufert, W. Auwärter, J. Schnadt, 'Iron phthalocyanine on Cu(111): Coverage-dependent assembly and symmetry breaking, temperature-induced homocoupling, and modification of the adsorbate-surface interaction by annealing', *J. Chem. Phys.* 144 **2016**, 94702.
- [32] K. Diller, F. Klappenberger, F. Allegretti, A. C. Papageorgiou, S. Fischer, A. Wiengarten, S. Joshi, K. Seufert, D. Ćija, W. Auwärter, J. V. Barth, 'Investigating the molecule-substrate interaction of prototypic tetrapyrrole compounds: Adsorption and self-metalation of porphine on Cu(111)', *J. Chem. Phys.* 138 **2013**, 154710.
- [33] M. Chen, M. Röckert, J. Xiao, H.-J. Drescher, H.-P. Steinrück, O. Lytken, J. M. Gottfried, 'Coordination Reactions and Layer Exchange Processes at a Buried Metal–Organic Interface', *J. Phys. Chem. C* 118 **2014**, 8501–8507.
- [34] M. Wahl, M. Stöhr, H. Spillmann, T. A. Jung, L. H. Gade, 'Rotation–libration in a hierarchic supramolecular rotor–stator system: Arrhenius activation and retardation by local interaction', *Chem. Commun.* **2007**, 1349–1351.
- [35] K. W. Hipps, X. Lu, X. D. Wang, U. Mazur, 'Metal d-Orbital Occupation-Dependent Images in the Scanning Tunneling Microscopy of Metal Phthalocyanines', *J. Phys. Chem.* 100 **1996**, 11207–11210.
- [36] X. Lu, K. W. Hipps, 'Scanning Tunneling Microscopy of Metal Phthalocyanines: d<sup>6</sup> and d<sup>8</sup> Cases', *J. Phys. Chem. B* 101 **1997**, 5391–5396.
- [37] L. E. Dinca, F. De Marchi, J. M. MacLeod, J. Lipton-Duffin, R. Gatti, D. Ma, D. F. Perepichka, F. Rosei, 'Pentacene on Ni(111): room-temperature molecular packing and temperature-activated conversion to graphene', *Nanoscale* 7 **2015**, 3263–3269.

- [38] K. Diller, F. Klappenberger, M. Marschall, K. Hermann, A. Nefedov, C. Wöll, J. V. Barth, 'Self-metalation of 2H-tetraphenylporphyrin on Cu(111): An x-ray spectroscopy study', *J. Chem. Phys.* **136** **2012**, 14705.
- [39] F. Buchner, K. Flechtner, Y. Bai, E. Zillner, I. Kellner, H.-P. Steinrück, H. Marbach, J. M. Gottfried, 'Coordination of Iron Atoms by Tetraphenylporphyrin Monolayers and Multilayers on Ag(111) and Formation of Iron-Tetraphenylporphyrin', *J. Phys. Chem. C* **112** **2008**, 15458–15465.
- [40] I. Horcas, R. Fernández, J. M. Gómez-Rodríguez, J. Colchero, J. Gómez-Herrero, A. M. Baro, 'WSXM: A software for scanning probe microscopy and a tool for nanotechnology', *Rev. Sci. Instrum.* **78** **2007**, 13705.
- [41] D. A. King, 'Thermal desorption from metal surfaces: A review', *Surf. Sci.* **47** **1975**, 384–402.
- [42] A. M. de Jong, J. W. Niemantsverdriet, 'Thermal desorption analysis: Comparative test of ten commonly applied procedures', *Surf. Sci.* **233** **1990**, 355–365.